Mobius3D

THE COMPLETE PATIENT QA SYSTEM

- **3D PATIENT PLAN QA**
- **3D IMRT/VMAT PRE TREATMENT QA**
- **3D *IN VIVO* DAILY TREATMENT QA**
- **ONLINE PATIENT POSITIONING QA**

Upgrade your patient safety by bridging the gap between patient QA and machine QA:

DoseLab, the complete TG-142 solution, is now integrated into Mobius3D!

Visit mobiusmed.com/mobius3d to learn more or register for a bi-weekly webinar at mobiusmed.com/webinars

MOBIUS MEDICAL SYSTEMS
INNOVATIVE SOFTWARE FOR MODERN RADIATION ONCOLOGY

Online dose reconstruction for tracked volumetric arc therapy: real-time implementation and offline quality assurance for prostate SBRT

Cornelis Ph. Kamerling,* Martin F. Fast,† Peter Ziegenhein, Martin J. Menten, Simeon Nill, and Uwe Oelfke
Joint Department of Physics, The Institute of Cancer Research and The Royal Marsden NHS Foundation Trust, London, SM2 5NG, UK
(Dated: August 15, 2017)

Purpose: Firstly, this study provides a real-time implementation of online dose reconstruction for tracked volumetric arc therapy (VMAT). Secondly, this study describes a novel offline quality assurance tool, based on commercial dose calculation algorithms.

Methods: Online dose reconstruction for VMAT is a computationally challenging task in terms of computer memory usage and calculation speed. To potentially reduce the amount of memory used, we analyzed the impact of beam angle sampling for dose calculation on the accuracy of the dose distribution. To establish the performance of the method, we planned two single-arc VMAT prostate stereotactic body radiation therapy cases for delivery with dynamic MLC tracking. For quality assurance of our online dose reconstruction method we have also developed a stand-alone offline dose reconstruction tool, which utilizes the RayStation treatment planning system to calculate dose.

Results: For the online reconstructed dose distributions of the tracked deliveries, we could establish strong resemblance for 72 and 36 beam co-planar equidistant beam samples with less than 1.2% deviation for the assessed dose-volume indicators (clinical target volume D98 and D2, and rectum D2). We could achieve average runtimes of 28–31 ms per reported MLC aperture for both dose computation and accumulation, meeting our real-time requirement. To cross-validate the offline tool we have compared the planned dose to the offline reconstructed dose for static deliveries and found excellent agreement (3%/3 mm global gamma passing rates of 99.8–100%).

Conclusion: Being able to reconstruct dose during delivery enables online quality assurance and online replanning strategies for VMAT. The offline quality assurance tool provides the means to validate novel online dose reconstruction applications using a commercial dose calculation engine.

I. INTRODUCTION

Online dose reconstruction aims at computing the actually delivered dose during radiation therapy, based on real-time treatment machine information and a patient motion model. The machine information consists of log files, which typically contain information on the actual dose rate, treatment head orientation and multi-leaf collimator (MLC) positions. Motion measurements can be utilized to continuously update a patient model, which allows for the computation of dose on a reference geometry. Reconstructing the delivered dose in real-time allows for online quality assurance and analysis of novel delivery techniques. Moreover, it paves the way for online re-planning approaches [1]. While offline dose reconstruction methods are well established [2–4], online techniques [5–8] are more challenging from a software engineering point of view. They require the implementation of high-speed, low-latency dose calculation methods and network interfaces between treatment machine and dose accumulation modules.

In a previous study we presented a novel in-house research software platform to facilitate online dose reconstruction and showed its applicability to assessing tracked step-and-shoot (S&S) deliveries for prostate stereotactic body radiation therapy (SBRT) [6]. In that study, MLC apertures were shifted in beams-eye-view (BEV) in real-time, based on actual measured tumor position data. The dose reconstruction platform was utilized to quantify the dosimetric effects of tumor tracking and to analyze the potential to reduce planning target volume (PTV) margins.

Our real-time dose calculation algorithm is based on pre-calculated dose-influence data, which is straightforward to compute for S&S intensity-modulated radiation therapy (IMRT). For volumetric arc therapy (VMAT), however, the linear accelerator (linac) irradiates continuously while the gantry is rotating. Consequently beam angles have to be approximated by a finite set of angles. Handling the considerably increased amount of dose-influence data compared to S&S IMRT is a challenging task in terms of memory usage and calculation speed. In this work we introduce an implementation of online dose reconstruction for VMAT and quantify the trade-off between the beam angle sampling and dosimetric accuracy.

We have created VMAT plans for two SBRT prostate patients. These plans were delivered on a research linac with and without dynamic MLC tracking. During delivery, motion monitoring was simulated and dose was reconstructed using our online tool for a variety of dose-influence beam sampling settings.

Our previous work on online dose reconstruction assessed MLC tracking scenarios for prostate [6] and lung SBRT [7]. The accuracy of this method could, however, not be investigated thoroughly due to the lack of a ref-

* corijn@gmail.com
† m.fast@nki.nl

erence dose reconstruction algorithm exploiting a similar motion model. To facilitate the validation of novel online dose reconstruction methods, we also present an offline dose calculation tool that utilizes dose engines from commercial treatment planning system (TPS). This offline tool relies on log files recorded during delivery and uses exactly the same information available to the online dose reconstruction and is similar to work from other groups [4, 9, 10]. It groups MLC apertures according to associated target positions and accumulates the dose for each motion bin separately utilizing RayStation (RaySearch, Stockholm, Sweden). We assessed our offline dose reconstruction tool by comparing planned dose to the offline reconstructed dose to confirm its validity. We then proceeded to use the offline reconstructed dose as a reference to benchmark different dose-influence beam sampling settings.

II. MATERIALS AND METHODS

A. Online dose reconstruction for VMAT

We previously reported on our in-house developed tracking and delivery software *DynaTrack* [11], which acts as a high-level control system for a research Synergy linac (Elekta AB, Stockholm, Sweden) equipped with an Agility 160 MLC. DynaTrack controls the radiation delivery through proprietary research interfaces provided by Elekta and receives the full machine state including leaf and jaw positions, gantry positions, dose rate, and elapsed cumulative monitor units every 40 ms. Moreover, DynaTrack can be connected to various motion acquisition systems to obtain real-time position information on anatomical features. The machine and patient geometry information is then advanced to our in-house research TPS *DynaPlan* [12] to enable dose reconstruction.

DynaPlan utilizes an adaptation of the fast dose calculation engine in *μKonRad* [13] to compute dose in real-time. The computation is based on beamlets, which describe the influence of a discrete rectangular segment of the fluence distribution on the patient dose. The dose contribution for an MLC aperture can be computed by converting the leaf positions, jaw positions and MUs to beamlet weightings. μKonRad was optimized to handle large sets of pre-calculated dose influence data on non-uniform memory access (NUMA) systems. The performance-critical data handling method in μKonRad as described in Ziegenhein *et al.* [13] was based on the libNUMA application programming interface (API), which is not portable to the Microsoft (Redmond, WA, USA) Windows operating system (OS). Since our online dose reconstruction platform is tailored to the Windows OS, the fast dose calculation engine had to be altered. First, we changed our parallel programming interface from OpenMP ([14]) to the Windows OS Threading API. This facilitates the communication with the dose reconstruction thread in DynaPlan. Apart from that the scheduling process of the operating system is directly accessible and events can be handled more efficiently. The same API also provides NUMA-sensitive memory pinning. Explicitely pinning data and threads to distinct memory domains is crucial on multi-processor systems to achieve optimal performance [15, p. 385]. To achieve maximal bandwidth the dose-influence data is distributed equally to all memory domains.

Patient geometry data can be directly imported into DynaPlan utilizing the IronPython scripting API from research RayStation v4.99. We have recently created the wrapper library *NativeRaystationConnect* (NRC) to make the API available in native C++ [16]. We have used the research RayStation dose-influence data exporter, which generates single-value decomposed (SVD) dose data for each beamlet.

Figure 1 describes the actual online dose reconstruction step-by-step, in line with our previous work in Fast *et al.* [6]. DynaTrack sends actual MLC apertures and target positions to DynaPlan immediately after they are available. DynaPlan is then polling for the apertures. Each received MLC aperture is matched to the target position closest in time. Then, the corresponding set of beamlets is identified based on the gantry angle. The geometrical overlap with the MLC aperture and the beamlet set results in a set of beamlet weights. We correct for the output fluence profile by multiplying the beamlet weights with the measured profile. Output factors are taken into account by approximating actual MLC apertures as a rectangular shape and subsequently applying Sterling's formula [17]. The corrections factors are based on the commissioned machine information as available in the RayPhysics module of RayStation. The processed beamlet weights are then sent to μKonRad, which computes the according dose contribution as a full 3D dose distribution. This contribution is subsequently multiplied by the incremental MUs delivered since the last reported aperture. As a last step the dose contribution is accumulated on the reference geometry using a simple motion model as introduced in Fast *et al.* [6]. To each target volume voxel in the reference geometry, the dose value of the corresponding voxel in the dose contribution is added, considering the target shift as reported by the corresponding target position. To all other voxels, the corresponding dose is added without application of a shift vector. Dose-volume indicators can be computed in real-time on the reference geometry.

B. Beam angle discretization

In our implementation of online dose reconstruction, we aim at performing the multiplication of the dose-influence data with the beamlet weights, i.e. the dose calculation, and the dose accumulation in less than 40 ms (in line with the linac interface update frequency as presented in Section II D) including overhead like data transport. Dose-influence data can be as large as 1 GB

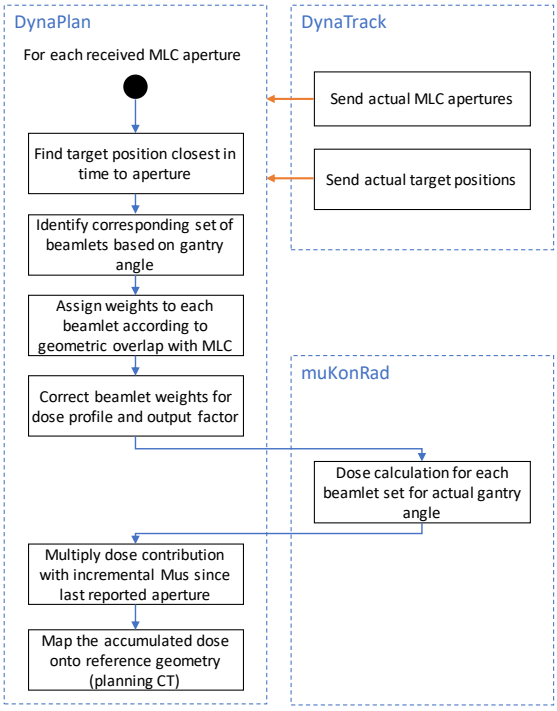

FIG. 1. Overview of the online dose computation triggered for each received MLC aperture.

per beam and hence the number of sampled beam angles is limited to the amount of random access memory (RAM) available. In this work we use co-planar equidistant sampling settings with a 5°, 10°, 20°and 40° gantry angle spacing, resulting in 72, 36, 18 and 9 sample points. We have implemented two dose reconstruction modes: *nearest neighbour* (NN) and *linear interpolation* (LI). In NN we compute the actual dose contribution by selecting the dose-influence data set closest to the actual gantry angle. To mitigate the discretization effect we explore the benefit of using a LI approach, in which the two nearest dose-influence data sets are chosen. The resulting dose contribution is then linearly interpolated from the two nearest-neighbour dose distributions based on the gantry angles. This method requires dose computation and accumulation twice per received MLC aperture.

C. Offline tool to validate online reconstructed doses

In order to validate the online reconstructed doses, an offline dose reconstruction tool was developed as part of this study. The tool is a stand-alone native C++ application, which imports DynaTrack log files (including delivery and target motion information) and supports both DicomRT[18] and NRC (c.f. Section II A) for data input/output. To include motion compensation in the accumulated dose, a simple patient model compensating for target shifts is adopted. This is the same method as in our online dose reconstruction platform, which is explained in Section II A.

Computing dose using a commercial dose computation algorithm in reasonable time requires various discretization steps. Figure 2 shows a flowchart describing the offline workflow. The tool processes delivery log files created by DynaTrack (a). This is exactly the same data as is processed in real-time in our online dose reconstruction tool. These log files contain the delivered MLC apertures (b) and the detected target positions (c). The tool groups target positions by discretization into 1 mm^3 motion bins (called patient geometry instances) based on the corresponding target position data (d). As a result, each MLC aperture is matched to the patient geometry it was delivered to (e). A log file typically contains thousands of MLC apertures. To make offline dose reconstruction feasible, these have to be merged into a workable set of apertures (f):

1. For each patient geometry instance, a beam ensemble is encoded by a set of S&S IMRT beams.

2. For a VMAT delivery such a beam ensemble can include up to a few hundred beams depending on beam angle sampling.

3. The large number of MLC apertures from the log file is reduced by merging similar apertures into a reduced discrete set of apertures based on a leaf position threshold of 0.5 mm. When merging apertures, the reported monitor units (MUs) are used to linearly interpolate the individual leaf positions.

In this study, NRC was utilized to compute the delivered dose in RayStation for each individual instance of patient geometry (g), using either the singular value decomposition (SVD) or collapsed cone (CC) dose engine. In a post-processing step, we shifted back the target dose onto the reference geometry (h) for each patient geometry instance, similar to the dose accumulation model for the online dose reconstruction platform as described in Section II A.

D. MLC tracking for VMAT

Previously, DynaTrack was used for either conformal deliveries [11], S&S IMRT [6], or conformal VMAT [19]. In this study, standard VMAT was supported for the first time. During VMAT delivery, both planned MLC leaf traversal and MLC tracking leaf motion occur simultaneously. If the original treatment plan requires fast leaf motion, maximum leaf speed might limit the ability to effectively correct for target motion. Therefore, the initial VMAT treatment DicomRT plan as generated by an arbitrary TPS must be modified to slow down gantry and leaf speed where required.

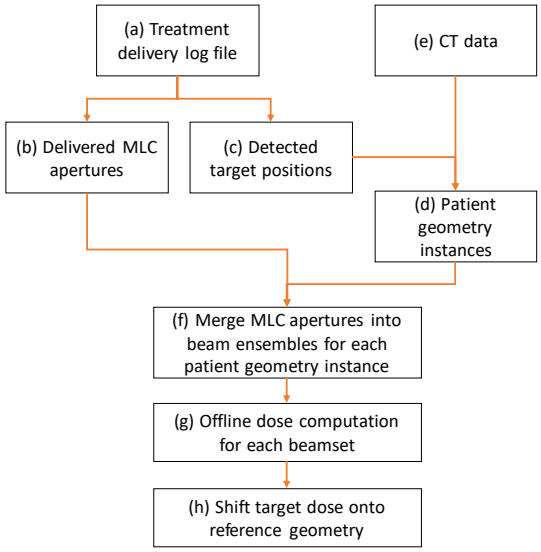

FIG. 2. Workflow chart describing the offline dose reconstruction tool.

Treatment plan conversion in DynaTrack is performed as follows. The initial VMAT treatment plan is first loaded onto the linac into Elekta's *stored-beam* delivery mode using the Elekta iCom interface. The linac control system then optimizes the VMAT delivery process based on plan parameters (e.g. leaf and jaw positions, gantry angles and monitor unit difference between adjacent control points as specified in the DicomRT plan file) and hardware constraints (e.g. maximum leaf and jaw speeds, maximum gantry speed and acceleration/deceleration, and maximum dose-rate). This initial optimization does not account for any additional leaf motion introduced through MLC tracking. In DynaTrack, we approximate the VMAT delivery optimization in Elekta's linac control system by re-implementing the VMAT delivery optimizer suggested by [20, 21]. In summary, the optimizer iteratively calculates the time difference, gantry speed, leaf and jaw speeds between adjacent plan control points, by starting of with the maximum permissible dose-rate and lowering the dose-rate in discrete steps until all speeds are within hardware constraints. The optimizer then considers the acceleration/deceleration behavior of the gantry and lowers the dose-rate further if necessary. Unlike [20, 21] we did not take *a priori* target trajectories into account when adapting the VMAT delivery optimizer for MLC tracking. Instead, we assumed a maximum target speed of 10 mm/sec to cover the vast majority of anatomical motion and lowered the maximum permissible leaf speed (35 mm/sec) and jaw speed (90 mm/sec) accordingly. In doing so we avoided having to synchronize the VMAT delivery with an *a priori* known target motion.

The VMAT plan modified in DynaTrack was then synchronized with Elekta's *stored-beam* delivery through the elapsed cumulative monitor units reported by the linac. DynaTrack continuously sends updated segments to the linac based on the convolution of plan segments with BEV target motion [22]. Crucially, it also sends the pre-calculated modified maximum dose-rates to the linac when appropriate to force the linac control system to adapt the gantry speed based on the actually achieved dose-rate. This avoids the complexity of implementing the complete gantry position and speed control in DynaTrack. For the treatment plans generated in this study, the adaptation of the VMAT delivery process only affected a minority of segments (those that came close to the maximum permissible speeds) and prolonged the overall treatment delivery by 3-5%.

E. Experimental setup

Figure 3 depicts all dose comparisons described in the following.

1. *Treatment planning and delivery modes*

We have assessed dose reconstruction for VMAT using patient data of two prostate SBRT cases, which have been used in a previous study [6]. Flattening-filter free (FFF) single-arc VMAT treatment plans were generated according to RTOG 0938, with a dose prescription of 5 $\times$ 7.25 Gy to 95% of the PTV. To generate the PTV, an isotropic 1 mm margin was added to the clinical target volume (CTV). This margin is smaller than proposed in the RTOG guideline, as we correct for intra-fractional motion using MLC tracking. Planning was performed in RayStation and the CC dose distribution (computed using a 2° gantry spacing) for each plan was saved to disk. The plans were delivered at a 1100 MU/min dose-rate using DynaTrack in the following modes:

Static delivery: Actual target position data is ignored for both delivery and dose accumulation. The resulting dose distribution is expected to match the planned dose distribution.

Tracked delivery: Actual target position data is used for MLC tracking and is incorporated in dose reconstruction. MLC tracking is expected to compensate for target motion and hence target dose is expected to be close to the planned dose distribution.

2. *Motion trajectory*

In this study target motion was simulated using a motion trajectory recorded by a previous study using the Calypso electromagnetic localization system [23]. This trajectory resulted in a dose deterioration without MLC

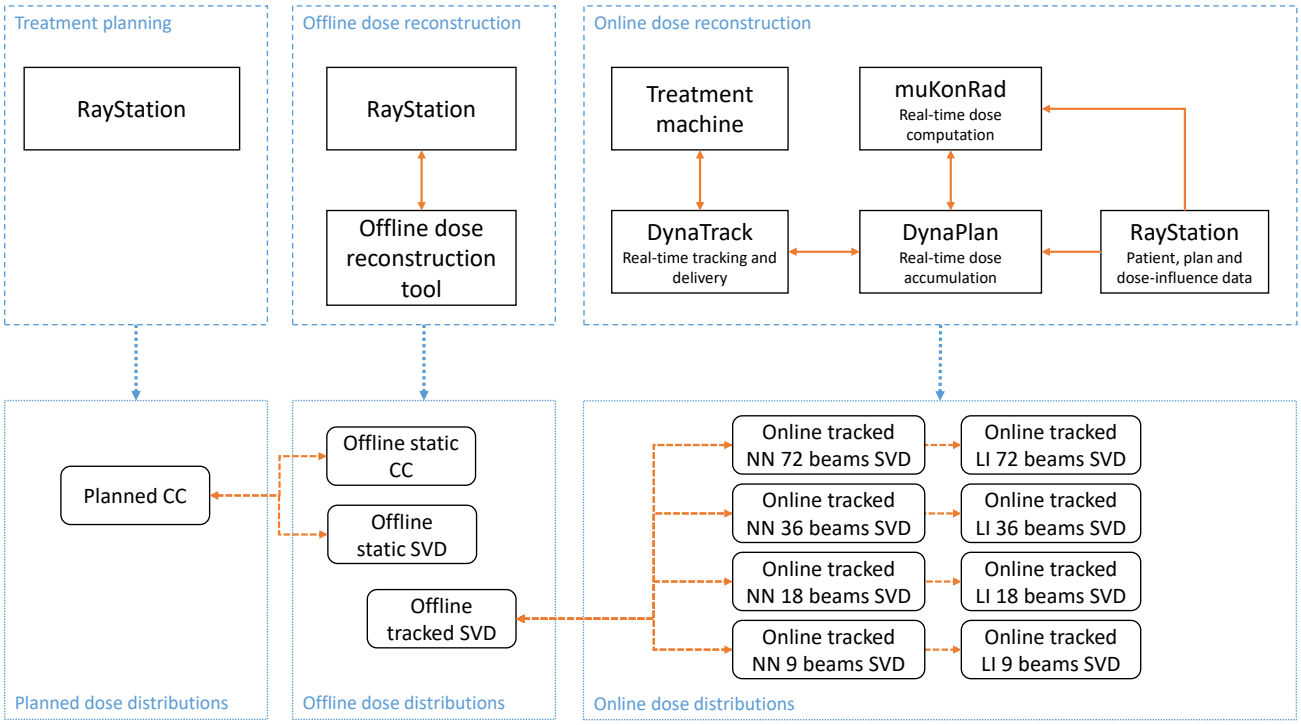

FIG. 3. Summary chart of the performed dose comparisons. The dashed blue boxes represent the three software environments used for computing dose distributions. The solid orange arrows represent system interfaces. The resulting dose distributions are listed in the dotted blue boxes. All dose comparisons are indicated by the dashed orange arrows.

tracking in our previous study in [6] and hence was selected as an example for this work. The trajectory consists of a slow baseline drift anteriorly and superiorly with sudden transient motion anteriorly and superiorly (high frequency). The trajectory is visualized in Figure 1(b) in Langen *et al.* [23].

3. *Validation of offline dose reconstruction*

We validated the log file acquisition, log file processing and dose computation by the offline dose reconstruction tool as introduced in Section II C by reconstructing statically delivered treatments and comparing the reconstructed dose distributions in both SVD and CC to the planned dose in CC. We have computed the global and local gamma passing rate: γ_g and γ_l (3%/3 mm) to assess dose deviations [24]. All voxels with less than 10% of the prescribed dose were ignored.

4. *Validation of online dose reconstruction*

We have validated the online dose reconstruction tool for tracked VMAT deliveries by comparing the real-time accumulated doses to the SVD dose distributions as generated in our offline dose reconstruction tool. The latter are referred to as *SVD reference* throughout this manuscript and were calculated on the same grid resolution as the online reconstructed dose. In the offline dose reconstruction tool, an equidistant beam angle sampling size of 2.5°was utilized for each patient geometry instance. We used the SVD dose engine for reference, as the exported dose-influence data is generated using the same engine. For online dose reconstruction, we have varied the number of sampled beams and the reconstruction mode as described in Section II B. Deviations from the SVD reference were assessed by computing γ_l and γ_g (3%/3 mm), CTV ΔD98 and ΔD2, rectum ΔD2 and the distributions of the per-voxel dose difference for the rectum volume. All voxels with less than 10% of the prescribed dose were ignored for the gamma comparison.

Dose-influence data was calculated independently for each sampled beam for the PTV plus a 2.5 cm isotropic expansion to cover the range of expected target motion. The dose influence data for 72 beams amounted to 56.6 GB for patient 1 and 77.7 GB for patient 2. The computed dose grid resolution was $2.1 \times 2.1 \times 1.5$ mm^3, and $1.9 \times 1.9 \times 1.3$ mm^3 respectively. We have computed the runtimes for computation and accumulation (including data transport overhead) of the 3D dose distribution for 60 slices centered around the isocenter for both patients and reconstruction modes, using all dose-influence data (i.e. with 5° beam spacing). The mean and 5%- and 95%-

percentiles were computed for the complete delivery.

5. Computer hardware

For this study, DynaPlan ran on an Intel (Santa Clara, CA, USA) Xeon E5-2697 v3 2.6 GHz in dual configuration with 128 GB main memory. DynaTrack ran on an Intel Xeon E5-2620 2.0 GHz. Both were compiled using Microsoft Visual Studio 2010/2012 and ran on the Microsoft Windows 7 OS. All high-performance algorithms were developed to run on Intel Xeon multi-core central processing unit (CPU) systems.

III. RESULTS

A. Dosimetric validation of offline dose reconstruction tool

The dosimetric analysis of the offline dose reconstruction tool is summarized in Table I. There is excellent agreement between the offline reconstructed dose and the planned dose distribution when the CC dose engine is used. For the SVD dose engine, offline reconstructed dose gamma passing rates were higher than 99.8% for γ_g and 83.3% for γ_l. Figure 4 shows dose-difference plots for the respective cases. The observed local dose differences were found to be less than 2% in and close to the target region. The maximum dose difference was -20 cGy (3% relative to the prescription dose), corresponding to the most red value and part of the skin dose.

B. Effects of beam angle discretization

The SVD reference was computed using the offline dose reconstruction tool. The motion binning resulted in 16 patient geometry instances for patient 1 and 14 instances for patient 2, respectively. The tool took about 30 minutes to reconstruct the dose for a single VMAT plan delivered with MLC tracking.

Figure 5 shows dose distributions for online reconstructed tracked deliveries for the different beam angle sampling settings in the left column. The discretization effect is visible especially for the lower-dose regions. Increasing the beam sampling increases the smoothness of the dose distribution. The right column presents dose difference maps, in which the online dose distributions are subtracted by the SVD reference.

The dose assessment of all online cases compared to the SVD reference are summarized in Table II. Global gamma passing rates γ_g are larger than 98.3% for all 36- and 72-beam cases. The coarser sampling results in gamma values dropping below 50% for the 9-beam cases. γ_l is consistently smaller than γ_g and is greater than 98.1% for all 72-beam cases. For most cases, γ_g and γ_l are slightly larger for LI compared to NN. The absolute dose differences for CTV ΔD98 and ΔD2 is less than 4.5 cGy (well below 1% relative to the prescription dose) for all cases, except for the 9-beam case, which shows deviations up to 15.5 cGy (2% relative to the prescription dose). The dose difference between ΔD98 and ΔD2 consistently increases while decreasing the beam sampling. The absolute rectum ΔD2 is 13.7 cGy at maximum (well below 2% relative to the prescription dose). Rectum ΔD2 slightly decreases when comparing LI to NN for most cases.

The distribution of the voxel-wise differences between the online reconstructed dose compared to the SVD reference is presented in the boxplots in Figure 6. The distributions for 72 and 36 beams are very similar. The absolute difference, however, increases slightly for 18 beams and more drastically for 9 beams. The distributions are marginally tighter for LI compared to NN.

C. Runtime analysis

Table III summarizes the runtimes for the full real-time computation required for each incoming MLC aperture in DynaPlan. The mean total runtime for NN ranged from 15.7–19.0 ms. The 95%-percentile for NN ranged from 21.7–35.0 ms. The mean total runtime for LI ranged from 28.0–31.0 ms. The 95%-percentile for LI ranged from 37.2–41.4 ms.

IV. DISCUSSION

We have successfully implemented an online dose reconstruction method for (tracked) VMAT deliveries which is suitable for prostate SBRT deliveries with MLC tracking. We have validated the method by comparing the online reconstructed dose distributions to the results of our newly proposed offline dose reconstruction tool, which is based on the dose engine of the RayStation TPS. For high beam-angle resolutions (72 and 36 beams) we have observed excellent agreement in both target and organ-at-risk (OAR) dose. The 18-beam sampling results in a decrease of accuracy in terms of local gamma pass-rate. However, the deviations of the assessed dose-volume points are still less than 1% compared to the dose prescription. Going to a 9-beam sampling clearly increases these deviations up to 2%. The absolute difference between CTV ΔD98 and ΔD2 increases for a decreasing beam sampling. This points at a less accurate sampling of the dose gradient, present at the target volume border. We could not establish a clear distinction between the NN and the LI dose reconstruction method.

The interpretation of the results depends largely on the application of online dose reconstruction. For online quality assurance, assessing target coverage only might be sufficient and hence a very coarse beam angle sampling might be acceptable. For more advanced applica-

TABLE I. Dosimetric comparison of offline reconstructed dose with planned dose

Patient	Offline static SVD		Offline static CC	
	γ_g [%]	γ_l [%]	γ_g [%]	γ_l [%]
1	99.8	83.3	100	93.9
2	99.8	91.7	100	99.2

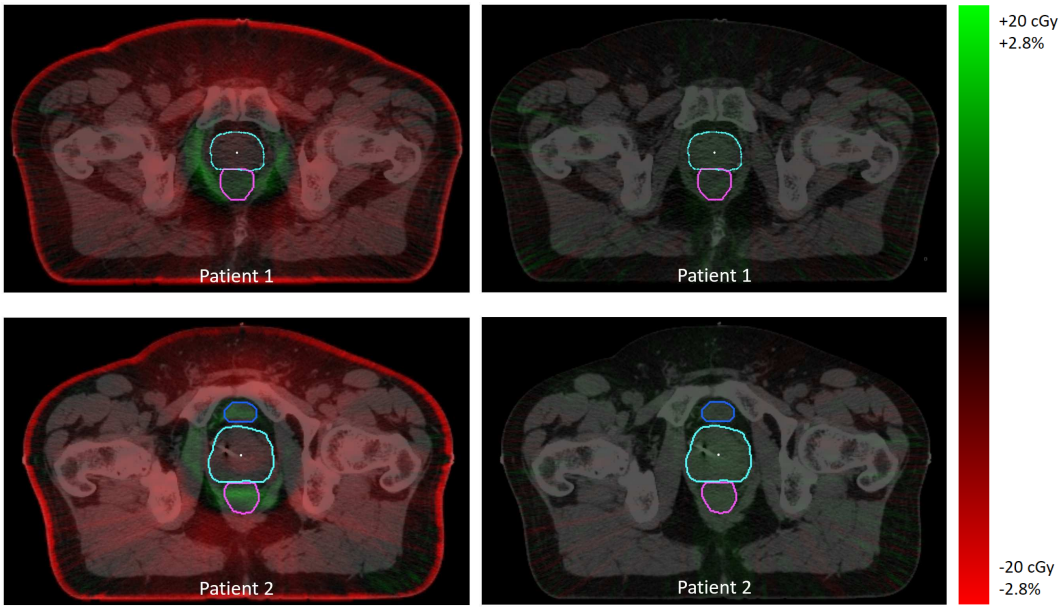

(a)Offline SVD (b)Offline CC

FIG. 4. Dose-difference maps show the similarity between offline reconstructed dose and the planned dose. Red corresponds to higher values in the planned dose distributions, green to lower values. The maximum dose difference was -20 cGy for the fraction dose (less than 3% of the prescription dose), corresponding to part of the skin dose. The relative numbers in the color bar correspond to the prescription dose of 7.25 Gy (100%).

tions like online replanning, dose-volume points are not a useful proxy for delivery quality as they have little significance for a partial irradiation. Instead, taking into account local dose differences is compulsory. Hence, we have presented the distribution of the voxel-wise differences in Figure 6. It can be clearly seen that a coarse beam sampling leads to high local dose errors in the rectal volume with a 95%-percentile up to 45 cGy (up to 6% relative to the prescription dose).

In addition to the online dose reconstruction work we have successfully implemented an offline dose reconstruction tool to validate online dose reconstruction using a commissioned dose engine. We have internally validated the offline dose reconstruction tool by comparing the planned dose (computed with RayStation's CC dose engine) with the offline reconstructed static dose. The gamma passing rates show excellent agreement with the offline reconstructed using the RayStation CC dose engine. We did observe residual errors of more than 3% local dose error in some beam entry regions, which consequently failed the gamma test. Additional analysis of the machine log files showed that these differences are caused by slight deviations in the planned and actually achieved machine states. Moreover, MLC aperture merging as described in Step (f) in Section II C results in additional deviations. The dose differences for offline reconstructed dose using the RayStation SVD dose engine were larger, but still within 2% for the target volume and surrounding tissue. We chose the SVD offline reconstructed dose as reference, as the dose-influence data can only be generated with RayStation's SVD engine. The offline dose reconstruction tool is crucial for quality assurance of future online dose reconstruction methods and its use extends beyond the specific application in this manuscript. In particular, external offline QA of our online dose reconstruction software will become increasingly important when more complex motion models and anatomy are considered. On top of the simple patient model correcting for target shifts, the offline dose reconstruction tool also supports 4D dose reconstruction using deformation vector fields and S&S IMRT.

The prostate SBRT patient cases were selected to assess the performance and accuracy of the presented online dose reconstruction method for VMAT. The method is not limited to prostate and could prove useful for other disease sites, e.g. for lung SBRT as we have shown in

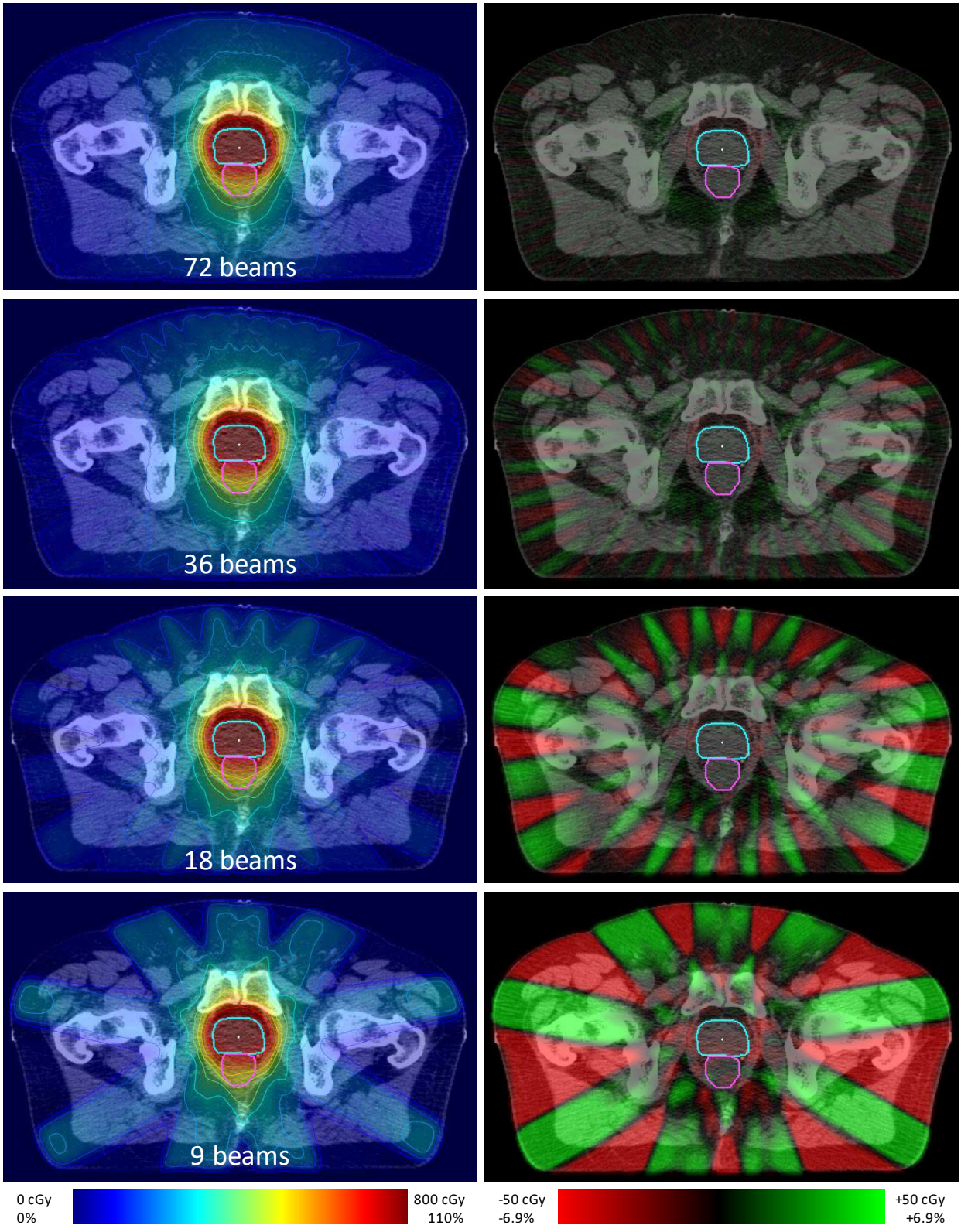

FIG. 5. The left column contains transversal dose distributions for online reconstructed tracked deliveries for the different beam angle sampling settings. The 10%-, 20%-, 30%-, 40%-, 50%-, 60%-, 70%-, 80%- and 90%-isodose lines are rendered.. The right column contains dose difference maps comparing the online reconstructed dose to the SVD reference. Please note that for the images on row three and four, the color scale is clipped. The maximum absolute difference is 73 cGy (10% relative to the prescription dose) for the 18-beam sampling and up to 105 cGy (14% relative to the prescription dose) for the 9-beam sampling. The relative numbers in the color bar correspond to the prescription dose of 7.25 Gy (100%). All dose distributions in this figure correspond to patient 2.

TABLE II. Dosimetric analysis of online dose reconstruction compared to SVD reference for tracked deliveries with 7.25 Gy dose prescription.

		Nearest Neighbor (NN)					Linear Interpolation (LI)				
Pat	Beams	γ_g [%]	γ_l [%]	CTV ΔD98 [cGy]	CTV ΔD2 [cGy]	Rec ΔD2 [cGy]	γ_g [%]	γ_l [%]	CTV ΔD98 [cGy]	CTV ΔD2 [cGy]	Rec ΔD2 [cGy]
1	72	100	96.7	-2.2	1.8	-3.0	100	97.3	-3.0	1.8	-3.0
	36	98.7	80.5	-3.0	1.8	-3.1	99.3	81.4	-3.0	1.8	-3.0
	18	81.4	55.0	-2.3	3.4	-4.0	81.8	55.5	-3.0	3.5	-3.9
	9	46.9	31.2	-13.3	-2.5	-13.3	46.8	31.2	-15.5	-1.9	-11.9
2	72	100	98.1	-4.4	0.3	-6.0	100	98.1	-4.4	0.3	-6.0
	36	98.4	86.2	-4.1	-1.2	-4.9	98.5	86.6	-3.1	0.6	-4.9
	18	83.8	60.0	-3.3	-3.2	-3.6	84.1	60.4	-2.9	3.6	-3.2
	9	51.6	36.3	-10.7	-3.8	-13.7	50.3	35.3	-6.0	1.3	-3.6

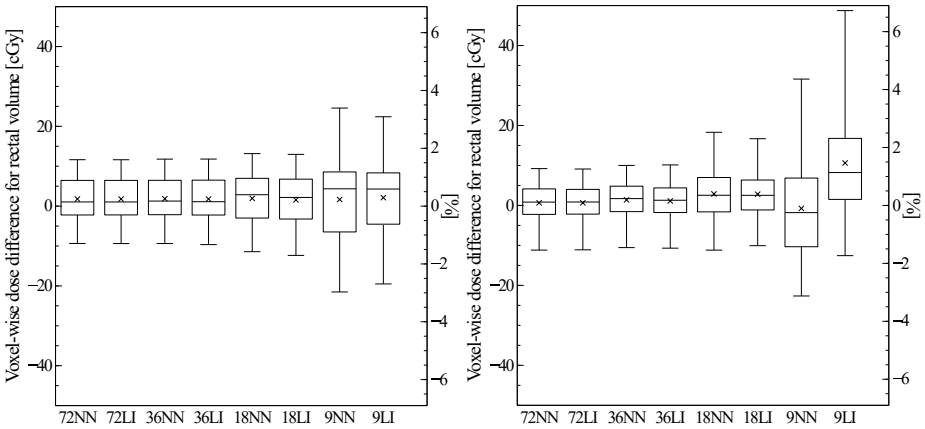

(a)Patient 1 (b)Patient 2

FIG. 6. Rectal volume voxel-wise dose differences (for the fraction dose) comparing online reconstructed dose to the SVD reference. The boxes represent the 25%-, 50%-, and 75%-percentile. The whiskers represent the 2%- and 98%- percentile. The crosses indicate the mean value. The relative numbers on the rights axes correspond to the prescription dose of 7.25 Gy (100%).

TABLE III. Total runtime per received MLC aperture [ms].

Patient	Nearest Neighbor (NN)			Linear Interpolation (LI)		
	5%-per	mean	95%-per	5%-per	mean	95%-per
1	11.8	15.7	21.7	22.4	28.0	37.2
2	12.9	19.0	35.0	24.8	31.0	41.4

Kamerling *et al.* [7] (for S&S IMRT). However, it should be mentioned that the geometry in this study should be considered simple compared to other disease sites. Therefore, the parameters used in this study can currently not be generalized to prove validity for all disease sites. The offline dose reconstruction tool as presented in this work, however, does not depend on the discretization we exploit in our online method and hence has the potential to validate our online dose reconstruction software when it is extended for more complex disease sites in the future.

We have successfully extended our tracking and delivery software DynaTrack to support standard VMAT deliveries. To make sure the maximum MLC leaf speed is not exceeded we have conservatively changed delivery dynamics such that additional motion as required for MLC tracking does not violate hardware constraints. An alternative approach might be to pause the beam delivery if the maximum leaf speed is exceeded. To fully quantify the benefit from MLC tracking, our proposed framework can be used to increase confidence in this and other novel delivery techniques. We have previously utilized the framework to assess the potential for margin reduction when MLC tracking is performed for prostate [6] and lung [7] SBRT in case study settings. To fully benefit from MLC tracking approaches, new planning strategies have to be explored using an increased amount of patient data.

Patient specific VMAT quality assurance based on offline dose reconstruction has mostly been performed without motion compensation [25–27] and is hence not suitable for tracked deliveries. Dose reconstruction for tracked VMAT deliveries should be considered essential, as recently patients have started undergoing first clinical trials using this delivery technique [10]. Poulsen *et al.* [4] have first proposed dose reconstruction incorporating motion compensation. Their motion model is correcting for target motion by shifting the plan isocenter, thus effectively shifting the entire CT with respect to the beam. Ravkilde *et al.* [9] presented a fast dose calculation method aiming at online dose reconstruction. However, the dose is computed using a simplified pencil-beam algorithm on two slices only. In contrast, our platform is capable of performing all computations online for the 3D volume, while not compromising on the quality of the dose engine. To accumulate the dose, both Poulsen *et al.* [4] and Ravkilde *et al.* [9] use the same motion model. Poulsen's method assumes that all surrounding organs-at-risk (OARs) move in line with the target, which is not necessarily correct for most treatment sites. Hence, OAR dose should be interpreted with care. The motion model in our online dose reconstruction platform shifts dose from the actual dose grid to a reference dose grid for the target volume only. In doing this, we assume that the anatomy surrounding the PTV is static. This assumption implies that e.g. the computed rectum D2 deviates from the delivered dose. However, this discrepancy does not influence the comparisons made in this work, as the same motion model was used for both offline and online computations. In contrast to Poulsen *et al.* [4] our motion model can be easily extended to include multiple structures of interest with different motion trajectories, respective real-time information becomes available.

It should be noted that our model should not be used in regions with large tissue inhomogeneities and/or deformations (e.g. lung), as the method assumes dose can be rigidly shifted in tissue. For such regions, more advanced motion models should be utilized, based on multiple images and corresponding non-rigid transformations, as e.g. described in Kamerling *et al.* [7], Glitzner *et al.* [28].

Other work proposing a solution for online dose reconstruction for S&S IMRT and VMAT was performed based on electronic portal imaging devices [5, 8]. This approach mainly aims at the detection of severe treatment errors, which may then result in halting the treatment delivery. In contrast, our software solution is able to compute 3D dose with a higher frequency and less latency using a motion model, which allows for real-time treatment plan adaptation instead of halting the linac. We have recently shown a proof-of-concept study for real-time replanning between beams [29], in which deviations from the planned dose are compensated for by replanning during actual treatment delivery, e.g. while the gantry is rotating during a S&S IMRT delivery. Intra-fractional replanning might compete with MLC tracking approaches, however further confidence in optimized delivered dose distributions might be gained by the synergy of these methods. Such novel approaches can only be investigated with online dose reconstruction software.

All dose distributions computed using RayStation (i.e. planned CC, offline static CC, offline static SVD and offline tracked SVD, c.f. Figure 3) were computed utilizing a beam angle sampling of 2.5°or finer. Tang *et al.* [30] and Otto [31] point out that accurate dose computation for VMAT plans requires beam angle sampling finer than 2.5°. We expect that for indications with relatively simple geometry, like prostate, increased accuracy is not expected [32]. When this work on VMAT online dose reconstruction is generalized to other disease sites, the required beam sampling has to be reconsidered per site. In contrast to the former studies, our work focuses on online dose reconstruction instead of forward dose calculation. We have therefore investigated the trade-off between computation time and dosimetric accuracy instead of aiming at maximal accuracy only.

To allow for real-time dose computation based on dose-influence data, the dose engine μKonRad, which was originally optimized for Unix-based systems, had to be ported to the Windows OS for integration into the online dose reconstruction software platform as described in [6, 7]. The implementation had to be optimized even further as described in Section II A to deal with the increased amount of dose-influence data as required for VMAT. As we were focused on establishing an upper bound of algorithmic performance, we have not tried to reduce the amount of dose-influence data per sampled beam. We directly used all the data as exported by

RayStation. We could observe memory throughputs of 65–85 GB/s, which is not far from the theoretical maximum bandwidth for the utilized CPU. The amount of data could potentially be decreased by a factor of three by applying dose-influence sampling methods [33]. This would decrease the amount of required RAM and speed up data loading times. As described in Ziegenhein *et al.* [13] the multiplication of the dose-influence data with beamlet weights is a memory-bound problem. Therefore, decreasing the total amount of memory is expected to further reduce the runtime per reported MLC aperture.

A. Summary and Conclusion

We have shown that online dose reconstruction for dynamic VMAT deliveries is technically feasible at a continuous rate of 25 Hz. We have shown that dose accuracy decreases for a decreased dose-influence beam sampling. For the prostate SBRT patient data and motion conditions in this study we could show very good agreement for 72- and 36-beam equidistant samplings, compared to the results of a separate offline dose reconstruction tool. Utilizing this tool enables offline quality assurance of novel online quality assurance methods using independent dose calculation software.

V. ACKNOWLEDGMENTS

We acknowledge support for the MLC tracking research from Elekta AB under a research agreement. Research at The Institute of Cancer Research is also supported by Cancer Research UK under Programme C33589/A19727. MFF is supported by Cancer Research UK under Programme C33589/A19908. We acknowledge NHS funding to the NIHR Biomedical Research Centre at The Royal Marsden and The Institute of Cancer Research.

CONFLICT OF INTEREST DISCLOSURE

The authors have no relevant conflicts of interest to disclose.

[1] CP Kamerling, MF Fast, P Ziegenhein, S Nill, and U Oelfke, "Th-cd-202-12: Online inter-beam replanning based on real-time dose reconstruction," Medical Physics **43** (2016).

[2] Anthony E. Lujan, Edward W. Larsen, James M. Balter, and Randall K. Ten Haken, "A method for incorporating organ motion due to breathing into 3d dose calculations," Medical Physics **26**, 715–720 (1999).

[3] Ben J Waghorn, Amish P Shah, Wilfred Ngwa, Sanford L Meeks, Joseph A Moore, Jeffrey V Siebers, and Katja M Langen, "A computational method for estimating the dosimetric effect of intra-fraction motion on step-and-shoot imrt and compensator plans," Physics in Medicine and Biology **55**, 4187 (2010).

[4] Per Rugaard Poulsen, Mai Lykkegaard Schmidt, Paul Keall, Esben Schjdt Worm, Walther Fledelius, and Lone Hoffmann, "A method of dose reconstruction for moving targets compatible with dynamic treatments," Medical Physics **39**, 6237–6246 (2012).

[5] Henry C. Woodruff, Todsaporn Fuangrod, Eric Van Uytven, Boyd M.C. McCurdy, Timothy van Beek, Shashank Bhatia, and Peter B. Greer, "First experience with real-time epid-based delivery verification during {IMRT} and {VMAT} sessions," International Journal of Radiation Oncology*Biology*Physics **93**, 516 – 522 (2015).

[6] M F Fast, C P Kamerling, P Ziegenhein, M J Menten, J L Bedford, S Nill, and U Oelfke, "Assessment of mlc tracking performance during hypofractionated prostate radiotherapy using real-time dose reconstruction," Physics in Medicine and Biology **61**, 1546 (2016).

[7] Cornelis Ph. Kamerling, Martin F. Fast, Peter Ziegenhein, Martin J. Menten, Simeon Nill, and Uwe Oelfke, "Real-time 4d dose reconstruction for tracked dynamic mlc deliveries for lung sbrt," Medical Physics **43**, 6072–6081 (2016).

[8] Hanno Spreeuw, Roel Rozendaal, Igor Olaciregui-Ruiz, Patrick Gonzlez, Anton Mans, Ben Mijnheer, and Marcel van Herk, "Online 3d epid-based dose verification: Proof of concept," Medical Physics **43**, 3969–3974 (2016).

[9] Thomas Ravkilde, Paul J Keall, Cai Grau, Morten Hyer, and Per R Poulsen, "Fast motion-including dose error reconstruction for vmat with and without mlc tracking," Physics in Medicine and Biology **59**, 7279 (2014).

[10] Emma Colvill, Jeremy T Booth, Ricky T O'Brien, Thomas N Eade, Andrew B Kneebone, Per R Poulsen, and Paul J Keall, "Multileaf collimator tracking improves dose delivery for prostate cancer radiation therapy: results of the first clinical trial," International Journal of Radiation Oncology* Biology* Physics **92**, 1141–1147 (2015).

[11] Martin F Fast, Simeon Nill, James L Bedford, and Uwe Oelfke, "Dynamic tumor tracking using the elekta agility mlc," Medical physics **41**, 111719 (2014).

[12] Cornelis Ph Kamerling, Peter Ziegenhein, Florian Sterzing, and Uwe Oelfke, "Interactive dose shaping part 2: proof of concept study for six prostate patients," Physics in Medicine and Biology **61**, 2471 (2016).

[13] Peter Ziegenhein, Cornelis Ph Kamerling, Mark Bangert, Julian Kunkel, and Uwe Oelfke, "Performance-optimized clinical imrt planning on modern cpus," Physics in Medicine and Biology **58**, 3705 (2013).

[14] Leonardo Dagum and Ramesh Menon, "Openmp: An industry-standard api for shared-memory programming," IEEE Comput. Sci. Eng. **5**, 46–55 (1998).

[15] Abraham Silberschatz, Peter Baer Galvin, and Greg Gagne, *Operating System Concepts*, 8th ed. (Wiley Publishing, 2008).

[16] CP Kamerling, P Ziegenhein, S Nill, and U Oelfke, "Ep-1440: Interfacing raystation in native c++: a novel methodology to utilise research software in a clinical setting," Radiotherapy and Oncology **115**, S778–S779 (2015).
[17] Theodor D Sterling, Harold Perry, and Leo Katz, "Automation of radiation treatment planningiv. derivation of a mathematical expression for the per cent depth dose surface of cobalt 60 beams and visualisation of multiple field dose distributions," The British journal of radiology **37**, 544–550 (1964).
[18] NEMA PS3 / ISO 12052, Digital Imaging and Communications in Medicine (DICOM) Standard, National Electrical Manufacturers Association, Rosslyn, VA, USA (available free at http://medical.nema.org/).
[19] James L Bedford, Martin F Fast, Simeon Nill, Fiona MA McDonald, Merina Ahmed, Vibeke N Hansen, and Uwe Oelfke, "Effect of mlc tracking latency on conformal volumetric modulated arc therapy (vmat) plans in 4d stereotactic lung treatment," Radiotherapy and Oncology **117**, 491–495 (2015).
[20] G A Davies, G Poludniowski, and S Webb, "Mlc tracking for elekta vmat: a modelling study," Physics in Medicine and Biology **56**, 7541 (2011).
[21] GA Davies, P Clowes, JL Bedford, PM Evans, S Webb, and G Poludniowski, "An experimental evaluation of the agility mlc for motion-compensated vmat delivery," Physics in medicine and biology **58**, 4643 (2013).
[22] Martin B Tacke, Simeon Nill, Andreas Krauss, and Uwe Oelfke, "Real-time tumor tracking: Automatic compensation of target motion using the siemens 160 mlc," Medical physics **37**, 753–761 (2010).
[23] K. M. Langen, T. R. Willoughby, S. L. Meeks, A. Santhanam, A. Cunningham, L. Levine, and P. A. Kupelian, "Observations on real-time prostate gland motion using electromagnetic tracking," Int. J. Radiat. Oncol. Biol. Phys. **71**, 1084–1090 (2008).
[24] Daniel A. Low and James F. Dempsey, "Evaluation of the gamma dose distribution comparison method," Medical Physics **30** (2003).
[25] Eduard Schreibmann, Anees Dhabaan, Eric Elder, and Tim Fox, "Patient-specific quality assurance method for vmat treatment delivery," Medical Physics **36** (2009).
[26] Benjamin E. Nelms, Daniel Opp, Joshua Robinson, Theresa K. Wolf, Geoffrey Zhang, Eduardo Moros, and Vladimir Feygelman, "Vmat qa: Measurement-guided 4d dose reconstruction on a patient," Medical Physics **39** (2012).
[27] Neelam Tyagi, Kai Yang, David Gersten, and Di Yan, "A real time dose monitoring and dose reconstruction tool for patient specific vmat qa and delivery," Medical Physics **39** (2012).
[28] M Glitzner, S P M Crijns, B Denis de Senneville, C Kontaxis, F M Prins, J J W Lagendijk, and B W Raaymakers, "On-line mr imaging for dose validation of abdominal radiotherapy," Physics in Medicine and Biology **60**, 8869 (2015).
[29] CP Kamerling, MF Fast, P Ziegenhein, S Nill, and U Oelfke, "Th-cd-202-12: Online inter-beam replanning based on real-time dose reconstruction," Medical Physics **43**, 3879–3879 (2016).
[30] Grace Tang, Matthew A Earl, Shuang Luan, Chao Wang, Daliang Cao, Cedric X Yu, and Shahid A Naqvi, "Stochastic versus deterministic kernel-based superposition approaches for dose calculation of intensity-modulated arcs," Physics in Medicine and Biology **53**, 4733 (2008).
[31] Karl Otto, "Volumetric modulated arc therapy: Imrt in a single gantry arc," Medical Physics **35** (2008).
[32] Karl Bzdusek, Henrik Friberger, Kjell Eriksson, Bjrn Hrdemark, David Robinson, and Michael Kaus, "Development and evaluation of an efficient approach to volumetric arc therapy planning," Medical Physics **36** (2009).
[33] Christian Thieke, Simeon Nill, Uwe Oelfke, and Thomas Bortfeld, "Acceleration of intensity-modulated radiotherapy dose calculation by importance sampling of the calculation matrices," Medical Physics **29** (2002).